A Novel Phenylaminotetralin Radioligand Reveals a Subpopulation of Histamine H_1 Receptors

RAYMOND G. BOOTH, NADER H. MONIRI, REMKO A. BAKKER, NEEPA Y. CHOKSI, WILLIAM B. NIX, HENK TIMMERMAN, and ROB LEURS

Division of Medicinal Chemistry and Natural Products, School of Pharmacy, University of North Carolina at Chapel Hill, Chapel Hill, North Carolina (R.G.B., N.H.M., N.Y.C., W.B.N.); and Leiden/Amsterdam Center for Drug Research, Division of Medicinal Chemistry, Vrije Universiteit, De Boelelaan, Amsterdam (R.A.B., H.T., R.L.)

ABSTRACT

Previously, (−)-*trans*-1-phenyl-3-*N*,*N*-dimethylamino-1,2,3,4-tetrahydronaphthalene ([−]-*trans*-H_2-PAT) was shown to activate stereospecifically histamine H_1 receptors coupled to modulation of tyrosine hydroxylase activity in guinea pig and rat forebrain in vitro and in vivo. Furthermore, the novel radioligand [^{3}H](−)-*trans*-H_2-PAT was shown to label selectively H_1 receptors in guinea pig and rat brain with high affinity (K_D, ~0.1 and 0.5 nM, respectively) and a B_{max} about 50 and 15%, respectively, of that observed for the H_1 antagonist radioligand [^{3}H]mepyramine. In the current study, [^{3}H](−)-*trans*-H_2-PAT-labeled cloned guinea pig and human H_1 receptors in Chinese hamster ovary (CHO) cell membranes with high affinity (K_D, ~0.08 and 0.23 nM, respectively) and a B_{max} about 15% of that observed for [^{3}H]mepyramine. The binding of H_2-PAT to H_1 receptors in both CHO-H_1 cell lines was stereoselective with the (−)-*trans*-isomer having affinity (K_i, ~1.5 nM) about 4-, 20-,

and 50-times higher than the (−)-*cis*-, (+)-*trans*-, and (+)-*cis*-isomers, respectively; the affinity of (−)-*trans*-H_2-PAT was unaffected by excess GTP. In functional assays, (−)-*trans*-H_2-PAT was a full antagonist of histamine H_1-mediated stimulation of phospholipase C (PLC) and [^{3}H]inositol phosphates (IP) formation in CHO-H_1 cells, a full inverse agonist of constitutively active H_1 receptors in COS-7-H_1 cells, and a full competitive antagonist (pA_2 = 9.2) of histamine H_1-mediated contraction of guinea pig ileum. It is concluded that (−)-*trans*-H_2-PAT is an antagonist at H_1 receptors coupled to PLC/IP formation and smooth muscle contraction. Meanwhile, the observation that [^{3}H](−)-*trans*-H_2-PAT labels only a subpopulation of H_1 receptors and that (−)-*trans*-H_2-PAT activates H_1 receptors coupled to modulation of tyrosine hydroxylase suggests that there may be post-translational H_1 receptor heterogeneity.

Previous studies in our laboratory showed that the lead compound in a series of novel 1-phenyl-3-amino-1,2,3,4-tetrahydronaphthalenes (PATs), (±)-*trans*-H_2-PAT (Fig. 1), stimulates tyrosine hydroxylase activity, rate-limiting in the synthesis of catecholamine neurotransmitters (i.e., dopamine and norepinephrine), in guinea pig and rat brain in vitro (Booth et al., 1993). Resolution of the enantiomers of (±)-*trans*-H_2-PAT (Wyrick et al., 1993) indicated that (−)-1*R*,3*S*-*trans*-H_2-PAT was the active isomer. Accordingly, [^{3}H](−)-*trans*-H_2-PAT (Fig. 1) was synthesized in our laboratories (Wyrick et al., 1994) for use in radioreceptor assays to characterize the receptor at which PATs might act to modulate catecholamine neurotransmitter synthesis in mammalian brain.

In guinea pig brain homogenate, [^{3}H](−)-*trans*-H_2-PAT

binds saturably (B_{max}, ~39 fmol/mg of protein) and with high affinity (K_D, ~0.1 nM) to a single population of sites (Booth et al., 1999). Competition binding studies and radioreceptor screening assays indicated that the pharmacological profile of [^{3}H](−)-*trans*-H_2-PAT sites is virtually identical to histamine H_1 receptors labeled with the standard H_1 antagonist radioligand [^{3}H]mepyramine (Fig. 1). Moreover, autoradiographic receptor mapping studies showed the guinea pig brain distribution of [^{3}H](−)-*trans*-H_2-PAT-labeled sites to be the same as histamine H_1 receptors labeled with [^{3}H]mepyramine (Booth et al., 1999), with both radioligands localizing mainly in forebrain structures dense in tyrosine hydroxylase-containing nerve terminals. Also, stimulation of tyrosine hydroxylase activity by (±)- and (−)-*trans*-H_2-PAT in guinea pig and rat brain in vitro is blocked by histamine H_1 receptor antagonists (Booth et al., 1993, 1999), similar to histamine H_1-mediated activation of tyrosine hydroxylase in bovine adrenal chromaffin cells (Marley and Robotis, 1998).

ABBREVIATIONS: PAT, 1-phenyl-3-amino-1,2,3,4-tetrahydronaphthalenes; GPCR, G protein-coupled receptor; CHO, Chinese hamster ovary; CHOgpH_1, CHO cells expressing cDNA for the guinea pig H_1 receptor; CHOhuH_1, CHO cells expressing cDNA for the human H_1 receptor; COShuH_1, African, green monkey kidney cells transfected with the human H_1 receptor; PLC, phospholipase C; IP, inositol phosphate; NF-κB, nuclear factor-κB; MEM, minimum essential medium; DMEM, Dulbecco's modified Eagle's medium.
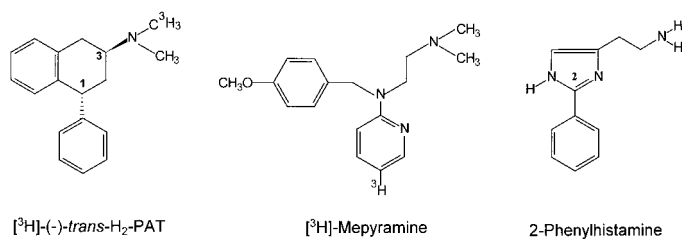
Fig. 1. H_2-PAT contains structural features associated with histamine H_1 agonists and antagonists.

The number of H_1 receptors labeled by $[^3H](-)$-$trans$-H_2-PAT in guinea pig brain, however, is only about 50% of the number labeled by $[^3H]$mepyramine (B_{max}, ~96 fmol/mg of protein).

As in guinea pig brain, in rat brain homogenate, $[^3H](-)$-$trans$-H_2-PAT also binds saturably (B_{max}, ~13 fmol/mg of protein), with high affinity (K_D, ~0.5 nM) to a single population of sites with a ligand binding profile that is virtually identical to histamine H_1 receptors labeled with $[^3H]$mepyramine (Choksi et al., 2000). The number of H_1 receptors labeled by $[^3H](-)$-$trans$-H_2-PAT, however, is only about 15% of the number labeled by $[^3H]$mepyramine (B_{max}, ~91 fmol/mg of protein). In vivo studies in rats showed that $(\pm)$-$trans$ H_2-PAT stimulates brain tyrosine hydroxylase activity and dopamine synthesis by a presynaptic receptor-mediated mechanism that is fully blocked by the H_1 antagonist triprolidine (Choksi et al., 2000). This effect of $(\pm)$-$trans$ H_2-PAT is very similar to the H_1-mediated stimulation of dopamine synthesis produced by histamine in rat brain in vivo (Fleckenstein et al., 1993). We proposed PATs as a novel class of H_1 ligands that activate presynaptic H_1 receptors coupled to modulation of tyrosine hydroxylase activity and catecholamine neurotransmitter synthesis in mammalian forebrain (Choksi et al., 2000).

Meanwhile, we have begun to examine why $[^3H](-)$-$trans$-H_2-PAT apparently distinguishes a subset of brain H_1 receptors. Rigorous analysis of ligands used to define nonspecific binding, buffers, number of membrane washings, and other technique-related possibilities have been eliminated. Although it is possible that $[^3H](-)$-$trans$-H_2-PAT may recognize an H_1 receptor subtype expressed in mammalian brain, molecular cloning evidence suggests there exists only a single H_1 gene product of the G protein-coupled receptor (GPCR) superfamily (Leurs et al., 1994; Traiffort et al., 1994). An alternative possibility in view of $(-)$-$trans$-H_2-PAT functional similarity to the endogenous agonist histamine regarding H_1-mediated activation of tyrosine hydroxylase is that $[^3H](-)$-$trans$-H_2-PAT is an H_1 receptor agonist radioligand. In such a case, $[^3H](-)$-$trans$-H_2-PAT may recognize only a subpopulation of H_1 receptors in a high-affinity state (e.g., already coupled to G protein) (De Lean et al., 1980). Interestingly, evaluation of the PAT pharmacophore indicates structural features common to both histamine H_1 antagonists and agonists. Specifically, H_2-PAT contains the diarylaminopropane structural moiety found in classical H_1 antagonists such as mepyramine (Fig. 1). Meanwhile, H_2-PAT also contains the appended phenyl substituent and imidazole-like aromatic character present in H_1 agonists of the 2-phenylhistamine type (Fig. 1) that are proposed to bind to H_1 receptors similarly to diarylaminopropane H_1 antagonists (ter Laak et al., 1995).

To characterize the H_1 binding characteristics and associated functional activity of PATs without the numerous confounding variables present in mammalian brain tissue (e.g., heterogeneity of neuroreceptors and downstream neurophysiological effects), we opted to use clonal cell lines stably transfected with cDNA encoding a single H_1-type receptor. Accordingly, herein we report the binding characteristics of $[^3H](-)$-$trans$-H_2-PAT in comparison to the standard H_1 antagonist radioligand $[^3H]$mepyramine in CHO cells expressing cDNA for the guinea pig (CHOgpH_1) (Traiffort et al., 1994) or human (CHOhuH_1) (Smit et al., 1996) H_1 receptor. We also examined PAT functional effects at H_1 receptors coupled to phospholipase C (PLC) and inositol phosphate (IP) formation in CHOgpH_1 cells (Leurs et al., 1994; Smit et al., 1996) and guinea pig ileum contraction (Leurs et al., 1991). For comparison, we evaluated PAT functional effects on constitutive H_1 receptor activity in African, green monkey kidney cells transfected with the human H_1 receptor (COShuH_1) (Bakker et al., 2000a) using an NF-κB reporter-gene bioluminescence assay (Bakker et al., 2000b, 2001).

Materials and Methods

Chemicals. $(\pm)$-$trans$-1-Phenyl-3-N,N-dimethylamino-1,2,3,4-tetrahydronaphthalene (H_2-PAT) was synthesized in a similar way to methods previously described (Wyrick et al., 1993). Briefly, the corresponding benzylstrylketone was cyclized to the tetralone intermediate and then reduced to the tetralol. This intermediate was tosylated, then converted to the free amine by reaction with sodium azide, and next followed by catalytic reduction to yield predominately the $(\pm)$-$trans$ isomer that was purified as the HCl salt. The racemic mixture was resolved by derivatization with $(-)$-camphorsulfonic acid to afford the more active $(-)$-$trans$-H_2-PAT enantiomer, which was subsequently radiolabeled with tritiated methyliodide to yield $[N$-methyl-$^3H]$-$(-)$-$trans$-H_2-PAT ($[^3H](-)$-$trans$-H_2-PAT; specific activity = 85 Ci/mmol) (Wyrick et al., 1994). $[^3H]$Mepyramine (30 Ci/mmol) was obtained from PerkinElmer Life Sciences (Boston, MA). D-Luciferin was purchased from Duchefa Biochemie BV (Haarlem, The Netherlands) and pNF-κB-Luc was from Stratagene (La Jolla, CA). Other compounds were obtained at the highest available purity from Sigma-Aldrich (St. Louis, MO) or Sigma/RBI (Natick, MA).

CHO Cell Culture. Studies were conducted with CHOgpH_1 (Traiffort et al., 1994) or CHOhuH_1 (Smit et al., 1996). Cells were grown to confluency in 75-cm² flasks containing α-minimum essential medium (with 4500 g/l glucose), supplemented with 10% fetal bovine serum, 2 mM L-glutamine, and 0.1% penicillin/streptomycin (100 units/100 μg/ml), in a humidified atmosphere of air/CO_2 (95:5%) at 37°C.

Radioligand Binding Assays Using CHO Cell Membranes. CHO cells were harvested by scraping from flasks with rinses (3 × 5 ml) of ice-cold phosphate-buffered saline (pH 7.5) and centrifuging at 1000g for 10 min. To prepare membranes, the resulting pellet was resuspended in 50 mM Na^+-K^+ phosphate buffer (pH 7.5; 25°C) at a volume of 1 ml/scraped flask. The suspension was homogenized using a Wheaton Teflon-glass homogenizer (Pittsburgh, PA) (10 strokes) and centrifuged at 50,000g (10 min, 4°C); the resulting pellet was resuspended in 50 mM Na^+-K^+ phosphate buffer (pH 7.5) at 1 ml/scraped flask (~800 μg of protein/ml) and stored at -80°C.

For saturation isotherms using CHO cell membranes, 100 μl of stock cell membrane homogenate described above was incubated for 30 min at 25°C with 0.01 to 7.0 nM $[^3H]$mepyramine or 0.01 to 1.0 nM $[^3H](-)$-$trans$-H_2-PAT in a total assay volume of 400 μl (50 mM Na^+-K^+ phosphate buffer). Nonspecific binding for both radioligands was defined by addition of 10 μM triprolidine. Results were analyzed by nonlinear regression using the rectangular hyperbola curve-fit-

ting algorithm in the microcomputer program Prism 3.0 (GraphPad, San Diego, CA) to determine K_D and B_{max}. Data were fit to one- and two-site models; however, no statistically significant (by F-test) improved fit was achieved using a two-site model. Each experimental condition was run in triplicate, and each experiment was repeated at least three times to determine S.E.M.

For competition binding assays using CHO cell membranes, 100 μl of the membrane preparation was incubated with 0.5 nM [³H]mepyramine or 0.1 nM [³H](−)-*trans*-H₂-PAT (about K_D) and 0.1 to 10,000 nM test ligand in a total assay volume of 400 μl (50 mM Na⁺-K⁺ phosphate buffer). Nonspecific binding was defined by the addition of 10 μM triprolidine for both radioligands. In assays where the effect of 1 mM GTP (Li₄⁺) on binding of ligands was measured, the buffer was 50 mM Tris HCl (pH 7.5) containing 4 mM MgCl₂.

Resulting inhibition data were analyzed by nonlinear regression using the sigmoidal curve-fitting algorithms in Prism 3.0 to determine concentration of competing ligands to inhibit specific binding of [³H](−)-*trans*-H₂-PAT by 50% (IC_{50}) and Hill slopes (n_H). Data were fitted to both one- and two-site models; however, no statistically significant (by F-test) improved fit was achieved using the two-site model. In light of the still, as yet, incompletely characterized nature of ligand interaction with the site, ligand affinity is expressed as an approximation of K_i values by converting IC_{50} data to $K_{0.5}$ values using the equation $K_{0.5} = IC_{50}/1 + L/K_D$, where L is the concentration of radioligand having affinity K_D (Cheng and Prusof, 1973). Each experimental condition was run in triplicate, and each experiment was performed a minimum of three times to determine S.E.M.

[³H]IP Formation in CHOgpH₁ Cells. Accumulation of [³H]IP was measured in CHOgpH₁ cells preincubated with [³H]myo-inositol, a precursor of the PLC substrate phosphatidylinositol. On the 3rd day of culture, confluent monolayers of CHOgpH₁ cells were rinsed 3 times with 5 ml of phosphate-buffered saline (pH 7.0; without Ca²⁺ and Mg²⁺). Trypsin (5 ml, 0.25%) was added, and cells were incubated at 37°C for 5 min. The cell suspension was then placed into a 15-ml conical tube, filled with α-minimum essential medium (MEM), and centrifuged at 1000*g* for 10 min. The resulting pellet was resuspended in α-MEM to obtain a cell density of approximately 1.8×10^5 cells/ml, as determined via bright-line hemocytometer. Aliquots (400 μl) of this suspension were added to each well of a polystyrene 12-well culture tray (approximately 7.0×10^4 cells/well). Trays were incubated overnight at 37°C.

After 16 to 20 h of incubation, CHOgpH₁ cells were confluent and adhered to wells. The trays were decanted, supplemented with 400 μl of α-MEM, and allowed to incubate at 37°C for 6 to 9 h. After this incubation period, medium was decanted, and each well was washed with 500 μl of inositol-free DMEM. After decanting of the inositol-free DMEM, a 400-μl suspension of [³H]myo-inositol in DMEM (inositol-free) was added to each well, yielding approximately 0.8 μCi of [³H]myo-inositol per well. After overnight incubation at 37°C, 100-μl aliquots of drug stocks containing 125 mM HEPES and 50 mM LiCl were added to triplicate wells (total well volume = 500 μl); trays were incubated in a 37°C water bath for 45 min. Medium was aspirated, trays placed on ice, and cell contents liberated upon addition of ice-cold 50 mM formic acid to each well. After 15 min on ice, formic acid was neutralized by the addition of 0.66 ml of 150 mM NH₄OH to each well. Well contents were added to individual AG1-X8 200-400 formate resin anion exchange columns (Bio-Rad Laboratories, Hercules, CA). Columns were washed with 10 ml of water, followed by 10 ml of 50 mM ammonium formate to displace any weakly attached anions. [³H]IP were eluted into scintillation vials upon addition of 5 ml of 1.2 M ammonium formate/0.1 M formic acid. Scintillation vials were counted for tritium by liquid scintillation spectroscopy using a Tri-carb 2100TR scintillation analyzer (Packard Instrument Co., Meriden, CT) at 65% counting efficiency; columns were regenerated upon addition of 5 ml of 2 M ammonium formate/0.1 M formic acid, followed by duplicate washes with 10 ml of water. Each experimental condition was run in triplicate. Data are mean percent basal control [³H]IP formation, and potency for hista-

mine is expressed as the concentration required to produce 50% maximal [³H]IP formation (EC_{50}) ± S.E.M. ($n \geq 3$), using the non-linear regression analysis algorithm in Prism 3.0. Statistical analysis was carried out using the Student's *t* test; *p* values < 0.05 were considered to indicate a significant difference.

COS-7 Cell Culture, Transfection, and Measurement of Inverse Agonism. COS-7 cells were grown at 37°C in a humidified atmosphere with 5% CO₂ in either DMEM containing 2 mM L-glutamine, 50 IU/ml penicillin, 50 μg/ml streptomycin, and 5% (v/v) fetal calf serum or with Glutamax I containing 50 IU/ml penicillin, 50 μg/ml streptomycin, and 0.5% (v/v) dialyzed fetal calf serum. Using the DEAE-dextran method (Brakenhoff et al., 1994), COS-7 cells were transiently transfected with either pcDEF₃ or pcDEF₃ containing the gene for the wild-type human histamine H₁ receptor (pcDEF₃hH₁) to yield 2.5 μg of pcDEF₃hH₁ and 12.5 μg of pNFκB-Luc/1 × 10⁷ cells (COShuH₁). Using this protocol, H₁-transfected (versus mock) cells show a high-affinity binding site for [³H]mepyramine, an increase in basal [³H]IP formation (consistent with H₁ receptor constitutive activity), and a selective concentration-dependent reduction in [³H]IP formation by H₁ receptor antagonists (consistent with H₁ receptor inverse agonist activity) (Bakker et al., 2000a,b, 2001).

To assess inverse agonism activity here, the transfected COShuH₁ cells were seeded (ca. 1 × 10⁵ cells/well) in 96-well blackplates (Costar, Cambridge, MA) in serum-free DMEM and incubated with the H₁ antagonist acrivastine or PATs (0.1–10,000 nM). After 48 h, cells were assayed for luminescence by aspiration of the medium followed by addition of 25 μl/well luciferase assay reagent (0.8 mM ATP, 0.8 mM D-luciferin, 19 mM MgCl₂, and 0.8 μM Na₂H₂P₂O₇) in 40 mM Tris (pH 7.8) buffer containing 0.4% (v/v) glycerol, 0.03% (v/v) Triton X-100, and 2.6 μM dithiothreitol. After 30 min, luminescence was measured for 3 s/well in a Victor² luminometer (Wallac-PerkinElmer, Brussels, Belgium). The basal luminescence of mock transfected cells was 13.7% of H₁-expressing cells. Data are expressed as mean percent basal control luminescence, and potency of PATs, mepyramine, acrivastine, and histamine is expressed as the concentration required to inhibit or stimulate basal control luminescence by 50% (IC_{50} or EC_{50}) ± S.E.M. ($n \geq 3$), using Prism.

H₁-Mediated Contraction of Guinea Pig Ileum. These assays were conducted similarly to methods previously reported (Leurs et al., 1991). Briefly, intestinal smooth muscle strips were prepared from male guinea pig ileum and mounted at 0.4 g of tension on a Hugo Sachs Hebel-Messovorsatz TL-2/HF-modem (Hugo Sach Electronik, Hugstetten, Germany) in 20 ml of Krebs buffer (117.5 mM NaCl, 5.6 mM KCl, 1.18 mM MgSO₄, 2.5 mM CaCl₂, 1.28 mM NaH₂PO₄, 25 mM NaHCO₃, and 5.5 mM glucose), continuously gassed with 95% O₂/5% CO₂ at 37°C. After equilibration for at least 45 min (fresh Krebs buffer replaced every 10 min), cumulative dose-contractile response curves were recorded using half-log increments of histamine. The contractile response produced by histamine was reevaluated after the addition (including a 5-min equilibration period) of (−)-*trans*-H₂-PAT (3.0–300 nM). Data are the mean percentage of contractile response, and potency is expressed as the concentration of histamine required to produce 50% maximal contractile response (EC_{50}) ± S.E.M. ($n \geq 3$) using Prism; antagonist potency of (−)-*trans*-H₂-PAT was quantified by Schild analysis.

Results

Binding Parameters of [³H](−)-*trans*-H₂-PAT and [³H]Mepyramine in CHO Cells. Wild-type (control) CHO cell membranes showed no measurable specific binding for [³H](−)-*trans*-H₂-PAT or [³H]mepyramine. On the other hand, in CHOgpH₁ membranes, [³H](−)-*trans*-H₂-PAT binds to an apparent single population of sites ($B_{max} = 44 \pm 2$ fmol/mg of protein) with high affinity ($K_D = 0.076 \pm 0.004$ nM); a representative saturation isotherm is shown in Fig.

2A. For comparison, we also examined the binding of the standard H_1 antagonist radioligand [³H]mepyramine, which also binds to an apparent single population of sites (B_{max} = 280 ± 10 fmol/mg of protein) with high affinity (K_D = 0.48 ± 0.03 nM) in CHOgpH_1 membranes (Fig. 2B). Similar results are obtained using membranes prepared from CHOhuH_1 cells (Fig. 3). [³H](−)-*trans*-H_2-PAT and [³H]mepyramine bind to an apparent single population of sites (B_{max} = 75 ± 8 and 578 ± 39 fmol/mg of protein, respectively) with high affinity (K_D = 0.23 ± 0.02 and 1.07 ± 0.04 nM, respectively) (Fig. 3, A and B, respectively). The difference observed in B_{max} values (ca. 6- to 8-fold) for specific binding of the two radioligands to CHOgpH_1 and CHOhuH_1 cell membranes are several times larger than the difference (ca. 2-fold) observed for guinea pig brain (Booth et al., 1999) and about the same as the difference (ca. 7-fold) observed in rat brain tissue (Choksi et al., 2000).

In another set of saturation binding experiments using CHOhuH_1 membranes, the two radioligands were tested side-by-side using concentrations of up to about 30-times K_D to reveal a possible additional binding site for [³H](−)-*trans*-H_2-PAT (Fig. 4). Data were fit to one- and two-site models; however, no statistically significant (by F-test) improved fit was achieved using a two-site model. Thus, an apparent
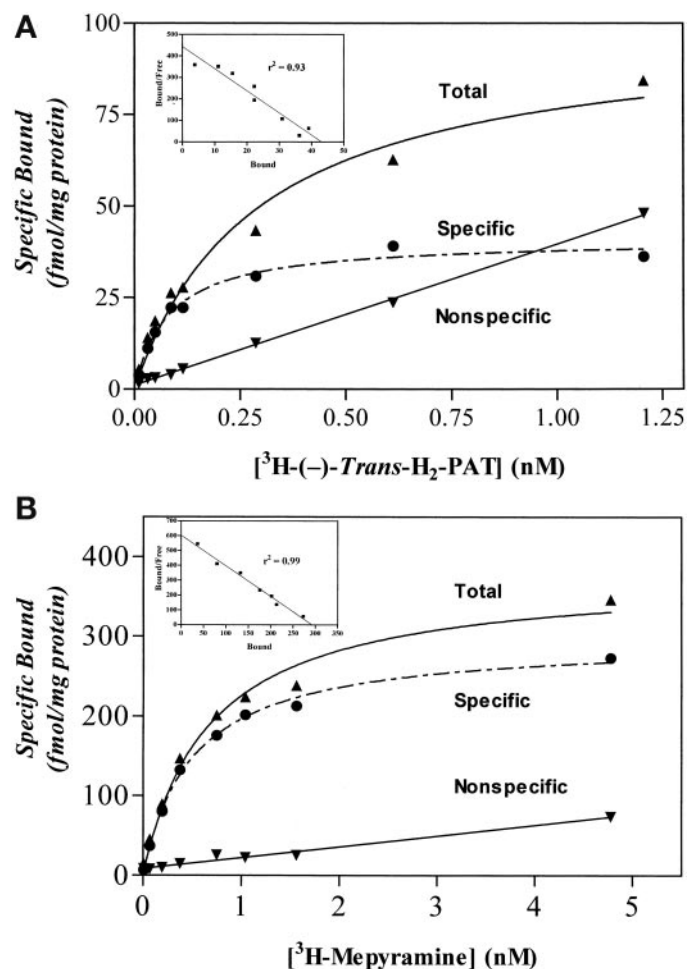
Fig. 2. Representative saturation isotherms and Scatchard plots of radioligand binding to CHOgpH_1 cells. A, [³H](−)-*trans*-H_2-PAT (B_{max} = 44 ± 2 fmol/mg of protein; K_D = 0.076 ± 0.004 nM); B, [³H]mepyramine (B_{max} = 280 ± 10 fmol/mg of protein; K_D = 0.48 ± 0.03 nM).
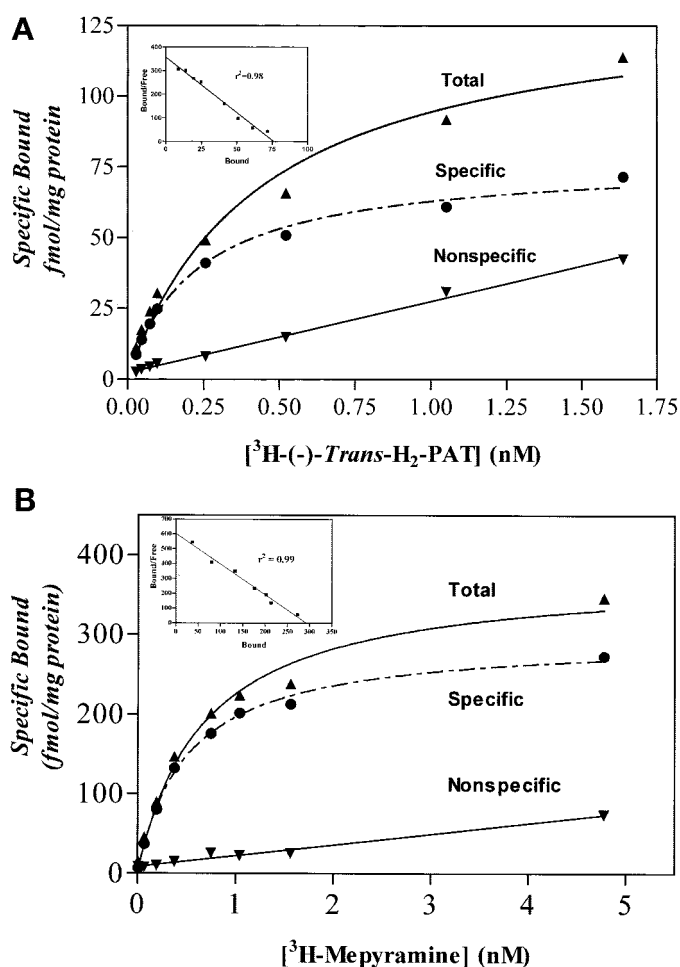
Fig. 3. Representative saturation isotherms and Scatchard plots of radioligand binding to CHOhuH_1 cells. A, [³H](−)-*trans*-H_2-PAT (B_{max} = 75 ± 8 fmol/mg of protein; K_D = 0.23 ± 0.02 nM); B, [³H]mepyramine (B_{max} = 578 ± 39 fmol/mg of protein; K_D = 1.07 ± 0.04 nM).
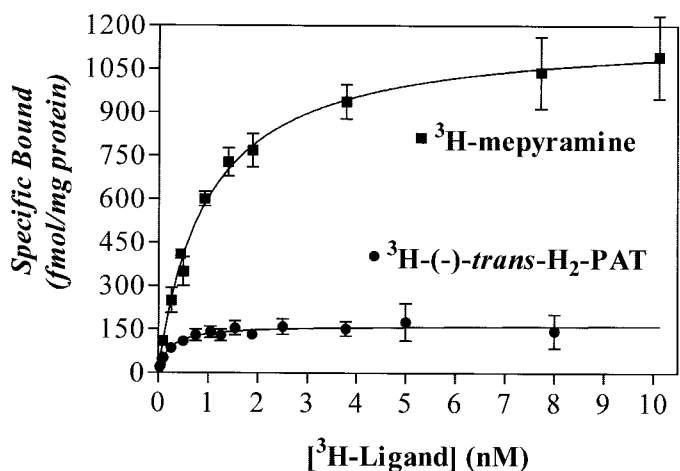
Fig. 4. [³H](−)-*trans*-H_2-PAT and [³H]mepyramine were tested side by side for specific binding to CHOhuH_1 membranes. Data were fit to one- and two-site models; however, no statistically significant (by F-test) improved fit was achieved using a two-site model. For [³H](−)-*trans*-H_2-PAT, K_D = 0.23 ± 0.05 nM and B_{max} = 160 ± 7.1 fmol/mg of protein. For [³H]mepyramine, K_D = 0.94 ± 0.09 nM and B_{max} = 1180 ± 30 fmol/mg of protein.

single population of H_1 receptors is revealed by each radioligand, and the B_{max} for specific binding of $[^3H](-)$-trans-H_2-PAT (160 ± 7.1 fmol/mg of protein) is about 14% of that observed for $[^3H]$mepyramine (1180 ± 30 fmol/mg of protein).

Radioligand Competition Binding Studies. Competition binding studies show that classical histamine H_1 antagonists ([+]-chlorpheniramine, diphenhydramine, mepyramine, and triprolidine) have high affinity ($K_{0.5}$, <15 nM; Table 1) for $[^3H](-)$-trans-H_2-PAT labeled and $[^3H]$mepyramine labeled sites in membranes prepared from $CHOgpH_1$ and $CHOhuH_1$ cells. Furthermore, the rank order of competition potency of characteristic H_1 ligands (i.e., doxepin > mepyramine ≥ triprolidine ≥ clozapine ≥ [+]-chlorpheniramine > diphenhydramine > [−]-chlorpheniramine > histamine; Table 1) is nearly identical when comparing $[^3H](-)$-trans-H_2-PAT to $[^3H]$mepyramine radiolabeling in $CHOgpH_1$ (r^2 = 0.90) and $CHOhuH_1$ (r^2 = 0.96) cells. These results are consistent with the H_1 receptor binding profiles of both radioligands in tissue from guinea pig (Booth et al., 1999) and rat (Choksi et al., 2000) brain.

The affinity of PATs for H_1 receptors labeled by either $[^3H](-)$-trans-H_2-PAT or $[^3H]$mepyramine in both CHO cell lines shows stereochemical preference identical to that observed in guinea pig (Bucholtz et al., 1998) and rat (Choksi et al., 2000) brain. As expected, trans-(1R,3S)-(−)-H_2-PAT ($K_{0.5}$, ~0.6–2 nM) shows the relatively highest affinity, whereas the corresponding trans-(1S,3R)-(+)-H_2-PAT enantiomer ($K_{0.5}$, ~12–40 nM) has about 20-fold lower affinity; racemic (±)-trans-H_2-PAT ($K_{0.5}$, ~1.4–4.3 nM) is near the theoretically predicted half-potency of the more active (−)-enantiomer. Meanwhile, the affinity of the cis-H_2-PAT enantiomers are severalfold lower than their corresponding trans-H_2-PAT diastereomers. The cis-(1S,3S)-(−)-H_2-PAT isomer ($K_{0.5}$, ~4–9 nM) has about 15-fold higher affinity than cis-(1R,3R)-(+)-H_2-PAT ($K_{0.5}$, ~54–130 nM), and the affinity of (±)-cis-H_2-PAT ($K_{0.5}$, ~8–15 nM) is about half the potency of the more active cis-(−)-enantiomer. Taken together, these results indicate that stereochemistry at the C1 phenyl group and especially at the C3 amino group (i.e., S configuration shared by both [−]-cis- and [−]-trans-H_2-PAT; Fig. 1) is important for PAT affinity at histamine H_1 receptors labeled

with either $[^3H](-)$-trans-H_2-PAT or $[^3H]$mepyramine in $CHOgpH_1$ and $CHOhuH_1$ cells.

Using either $[^3H](-)$-trans-H_2-PAT or $[^3H]$mepyramine as the radioligand, competition binding curves for most tested ligands were sigmoidal shaped with Hill (n_H) coefficients close to unity (Table 1), expected from ligands that bind competitively (presumably as antagonists) to a single population of receptors. Competition with histamine, however, gave a shallow sloped (n_H, ~0.7) concentration-response curve characteristic of agonist ligand binding at G protein-coupled receptors, according to the ternary complex model with limiting availability of G protein (De Lean et al., 1980). Virtually full displacement of either radioligand could be achieved by all tested ligands in either cell line. Radioligand displacement curves for representative ligands in Table 1 in competition for $[^3H]$mepyramine labeled H_1 receptors in $CHOhuH_1$ membranes are shown in Fig. 5. Data were fit to one- and two-site models; however, no statistically significant (by F-test) improved fit was achieved using a two-site model.

The ternary complex model also predicts the so-called "GTP-shift" (i.e., lower agonist ligand affinity is obtained in the presence of excess GTP as a result of virtually all receptors being converted to a G protein-uncoupled state). To investigate differences in functional binding that may occur between $[^3H]$mepyramine and $[^3H](-)$-trans-H_2-PAT at H_1 receptors, we examined the effect of excess GTP (1 mM) on the competitive binding of the H_1 antagonist (+)-chlorpheniramine, (−)-trans-H_2-PAT, and histamine. The $CHOgpH_1$ cell line was used for these studies since these cells also were used to measure H_1-mediated functional effects on IP formation (vide infra). There was no significant difference (p > 0.05) in affinity observed for (+)-chlorpheniramine or (−)-trans-H_2-PAT, with or without excess GTP, using either radioligand. Meanwhile, the affinity of histamine was significantly (p < 0.02) reduced with excess GTP using either $[^3H]$mepyramine ($K_{0.5}$, ~18 versus 25 μM, with and without excess GTP, respectively; Table 1) or $[^3H](-)$-trans-H_2-PAT ($K_{0.5}$, ~10 versus 18 μM, with and without excess GTP, respectively; Table 1). The ~1.5- to 2-fold increase in K_i values for histamine in the presence of GTP is similar to results reported using guinea pig brain homogenates (Chang

TABLE 1
Affinity of ligands for $[^3H]$-mepyramine and $[^3H]$-(−)-trans-H_2-PAT labeled H_1 receptors in $CHOgpH_1$ and $CHOhuH_1$ cell membranes

Ligand	CHOgpH$_1$ $K_{0.5}$				CHOhuH$_1$ $K_{0.5}$			
	vs. $[^3H]$-Mepyramine	n_H	vs. $[^3H]$-(−)-trans-H_2-PAT	n_H	vs. $[^3H]$-Mepyramine	n_H	vs. $[^3H]$-(−)-trans-H_2-PAT	n_H
	nM				*nM*			
Doxepin	0.28 ± 0.01	1.04 ± 0.07	0.16 ± 0.02	1.16 ± 0.15	0.32 ± 0.01	1.15 ± 0.06	0.09 ± 0.01	0.91 ± 0.09
Mepyramine	0.57 ± 0.01	0.84 ± 0.03	0.74 ± 0.05	1.05 ± 0.04	1.18 ± 0.10	1.05 ± 0.07	1.01 ± 0.04	1.13 ± 0.13
Triprolidine	0.93 ± 0.16	0.92 ± 0.08	0.69 ± 0.07	1.06 ± 0.10	1.53 ± 0.12	0.98 ± 0.02	1.11 ± 0.06	1.03 ± 0.12
(+)-Chlorpheniramine	1.98 ± 0.16	0.97 ± 0.04	0.69 ± 0.10	0.93 ± 0.02	4.81 ± 0.05	0.99 ± 0.06	2.67 ± 0.23	0.92 ± 0.06
(−)-Chlorpheniramine	98.0 ± 1.0	0.96 ± 0.06	80.1 ± 7.4	0.92 ± 0.04	361 ± 40	1.03 ± 0.07	211 ± 9	0.91 ± 0.07
Diphenhydramine	9.20 ± 0.81	0.87 ± 0.01	9.57 ± 0.79	1.31 ± 0.04	13.5 ± 1.0	0.97 ± 0.04	11.7 ± 0.75	0.89 ± 0.11
Clozapine	1.23 ± 0.03	0.98 ± 0.02	2.07 ± 0.13	1.29 ± 0.20	1.63 ± 0.15	1.07 ± 0.18	1.54 ± 0.11	1.27 ± 0.13
(−)-trans-H_2-PAT	1.15 ± 0.36	0.87 ± 0.14	0.58 ± 0.10	0.96 ± 0.03	2.50 ± 0.17	0.91 ± 0.09	1.65 ± 0.14	0.98 ± 0.11
(±)-trans-H_2-PAT	1.53 ± 0.06	0.98 ± 0.03	1.37 ± 0.04	0.95 ± 0.11	4.26 ± 0.25	0.89 ± 0.07	2.49 ± 0.27	0.98 ± 0.13
(+)-trans-H_2-PAT	23.0 ± 2.0	1.03 ± 0.06	11.54 ± 0.13	1.14 ± 0.15	42.4 ± 1.6	1.04 ± 0.06	29.9 ± 4.7	1.02 ± 0.09
(−)-cis-H_2-PAT	3.92 ± 0.18	0.86 ± 0.07	4.91 ± 0.03	1.03 ± 0.08	8.91 ± 0.76	0.89 ± 0.08	6.31 ± 0.23	0.92 ± 0.05
(±)-cis-H_2-PAT	10.89 ± 0.14	1.00 ± 0.02	7.87 ± 0.63	1.14 ± 0.02	13.6 ± 0.8	0.88 ± 0.02	14.7 ± 0.46	1.00 ± 0.01
(+)-cis-H_2-PAT	53.79 ± 1.39	0.97 ± 0.04	77.7 ± 1.07	1.23 ± 0.18	129 ± 13	0.87 ± 0.07	122 ± 9	1.00 ± 0.13
Histamine	18.3 ± 1.2 μM	0.72 ± 0.09	9.9 ± 0.9 μM	0.65 ± 0.05	13.5 ± 0.8 μM	0.67 ± 0.01	10.5 ± 0.6 μM	0.72 ± 0.03
+1 mM GTP	25.0 ± 1.5 μM	0.85 ± 0.09	17.6 ± 0.9 μM	0.78 ± 0.09	N.D.		N.D.	

N.D., not determined.
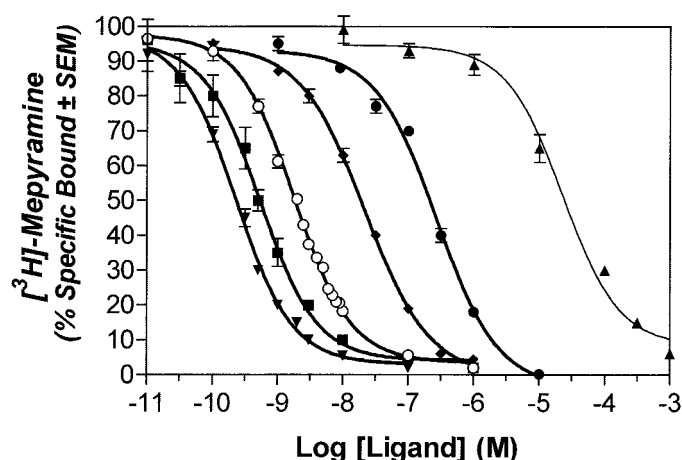
Fig. 5. Representative ligand concentration-radioligand displacement curves for several ligands in Table 1. ▼, doxepin; ■, mepyramine; ○, (−)-*trans*-H$_2$-PAT; ◆, diphenhydramine; ●, (+)-*cis*-H$_2$-PAT; ▲, histamine.

and Snyder, 1980). As expected, the Hill coefficient (n_H) for histamine significantly ($p < 0.05$) increased from about 0.7 to 0.8 in the presence of excess GTP (Table 1), suggesting binding occurred to a single population of low-affinity G protein-uncoupled H$_1$ receptors.

[^{3}H]IP Formation in CHOgpH$_1$ Cells. Previously, it was reported that stimulation of H$_1$ receptors on CHOgpH$_1$ (and CHOhuH$_1$) cells leads to activation of PLC and increased production of IP (Leurs et al., 1994; Smit et al., 1996). In the current studies, histamine produced a concentration-dependent stimulation of [^{3}H]IP formation in CHOgpH$_1$ cells preincubated with [^{3}H]myo-inositol (Fig. 6), consistent with the literature. Maximal stimulation was observed to be about 900% of basal control [^{3}H]IP formation at about 100 μM histamine (EC$_{50}$ = 2.6 ± 0.2 μM; $n = 4$).

Antagonism of Histamine-Induced Stimulation of [^{3}H]IP Accumulation. Triprolidine, (+)- and (−)-*cis*-H$_2$-PAT, and, (+)- and (−)-*trans*-H$_2$-PAT also were tested for effects on [^{3}H]IP accumulation in CHOgpH$_1$ cells. At concentrations spanning 0.01 to 10 μM, none of these H$_1$ ligands increased [^{3}H]IP accumulation over the basal level (data not shown). Thus, it was concluded that the PATs, like triproli-

dine, are not agonists at H$_1$ receptors coupled to IP formation. Test compounds subsequently were assessed for ability to antagonize the effect of histamine (3 μM, about EC$_{50}$) to stimulate [^{3}H]IP accumulation. As summarized in Fig. 7, histamine-induced [^{3}H]IP accumulation was essentially fully blocked by 1.0 μM of the H$_1$ antagonist triprolidine (percentage of the control histamine response = 4.1 ± 0.3) and (−)-*trans*-H$_2$-PAT (percentage of the control histamine response = 2.8 ± 0.1). Comparatively, the histamine effect was incompletely antagonized by 1.0 μM (−)-*cis*-, (+)-*trans*-, and (+)-*cis*-H$_2$-PAT (percentage of the control histamine response = 16.6 ± 1.0, 26 ± 1.0, and 65 ± 1.3; respectively); at 10 μM, however, these PATs fully blocked the histamine effect (percentage of the control histamine response = 0.6 ± 1.1, 2.1 ± 1.4, and 2.1 ± 1.3; respectively). In comparison to triprolidine and (−)-*trans*-H$_2$-PAT, the higher concentration of (−)-*cis*-, (+)-*trans*-, and (+)-*cis*-H$_2$-PAT required to fully antagonize histamine-induced stimulation of [^{3}H]IP accumulation is consistent with their lower affinity for H$_1$ receptors in CHOgpH$_1$ cells (Table 1).
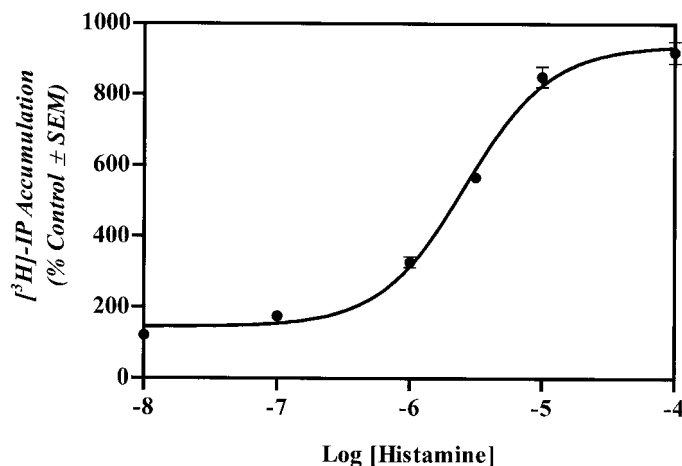
Effect of PATs on Constitutive H$_1$ Receptor Activity (Inverse Agonism) in COS-7 Cells. Recently, constitutive histamine H$_1$ receptor activity was shown in COS-7 cells transiently transfected with the human H$_1$ receptor (COShuH$_1$) (Bakker et al., 2000a, 2001). Here, we evaluated PAT functional responses in COShuH$_1$ cells using the NF-κB reporter-gene assay that measures H$_1$ receptor-mediated bioluminescence (Bakker et al., 2000b, 2001). The H$_1$ antagonists mepyramine and acrivastine and the endogenous agonist histamine were used as reference compounds in this assay. The basal luminescence of mock transfected cells was 13.7% of H$_1$-expressing cells. Constitutive H$_1$ receptor activity in COShuH$_1$ cells, as measured by luminescence, is inhibited (versus basal control) by mepyramine (IC$_{50}$ = 20.7 ± 0.7 nM) and acrivastine (IC$_{50}$ = 60 ± 0.5 nM) (Fig. 8). This activity of known H$_1$ antagonists has been interpreted as

Fig. 6. H$_1$ receptor-mediated stimulation of [^{3}H]IP accumulation in CHOgpH$_1$ cells by histamine. Maximal stimulation of basal [^{3}H]IP accumulation is 940 ± 40% at 100 μM; EC$_{50}$ = 2.6 ± 0.2 μM.
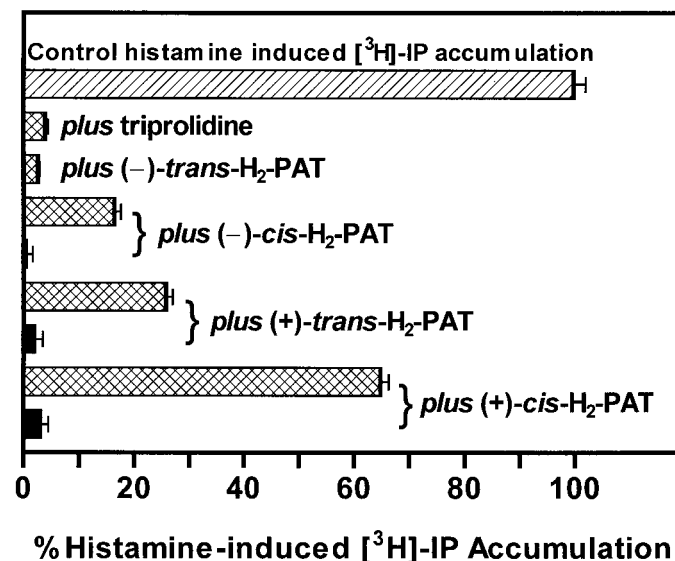
Fig. 7. Antagonism of histamine (3 μM) induced [^{3}H]IP accumulation in CHOgpH$_1$ cells. At 1.0 μM (thatched bars), triprolidine and (−)-*trans*-H$_2$-PAT fully blocked, and the other PAT isomers significantly ($p < 0.05$) reduced, the histamine effect; at 10 μM (solid bars), (−)-*cis*- (+)-*trans*- and (+)-*cis*-H$_2$-PAT fully blocked the histamine effect. Antagonists alone had no effect on [^{3}H]IP accumulation (data not shown).
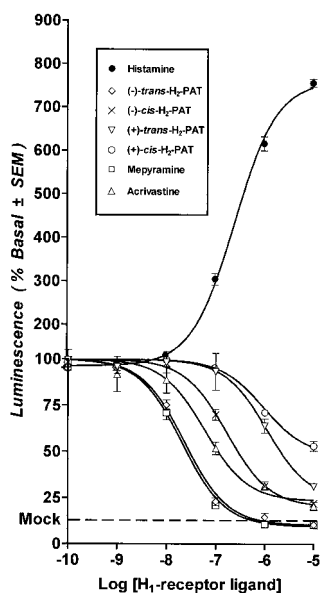
Fig. 8. Constitutive H_1 receptor activity (inverse agonism) as measured by inhibition of basal luminescence in COShuH$_1$ cells. Maximal inhibition by the reference compound acrivastine is $79.8 \pm 2.3\%$ at 100 μM; IC$_{50}$ = 40 ± 0.5 nM.

inverse agonism (Bakker et al., 2000a,b, 2001). Conversely, the endogenous agonist histamine stimulates (EC$_{50}$ = 250 $\pm$ 10 nM) H_1 receptor activity and luminescence. As shown in Fig. 8, all the PAT isomers also inhibited constitutive H_1 receptor activity in this assay with the following potency order: $(-)$-*trans*-H$_2$-PAT (IC$_{50}$ = 23 $\pm$ 0.4 nM) > $(-)$-*cis*-H$_2$-PAT (IC$_{50}$ = 170 $\pm$ 2 nM) > $(+)$-*cis*-H$_2$-PAT (IC$_{50}$ = 940 $\pm$ 30 nM) > $(+)$-*trans*-H$_2$-PAT (IC$_{50}$ = 1100 $\pm$ 21 nM). Consistent with its low H_1 binding potency (Table 1), $(+)$-*cis*-H$_2$-PAT did not fully inhibit basal luminescence even at 100 μM (about the limit of its solubility). These results indicate that the PATs behave functionally similarly to classical H_1 antagonists or inverse agonists (mepyramine and acrivastine) and not like the agonist histamine in this assay system.

We also determined the affinity of the PATs for [^{3}H]mepyramine-labeled H_1 receptors in membrane preparations from the COShuH$_1$ cell line. The rank order of affinity of PAT isomers is consistent with their rank order of functional potency in COShuH$_1$ cells (see above), i.e., $(-)$-*trans*-H$_2$-PAT ($K_{0.5}$ = 2.0 $\pm$ 0.01 nM) > $(-)$-*cis*-H$_2$-PAT ($K_{0.5}$ = 7.0 $\pm$ 0.02 nM) > $(+)$-*trans*-H$_2$-PAT ($K_{0.5}$ = 54 $\pm$ 0.3 nM) > $(+)$-*cis*-H$_2$-PAT ($K_{0.5}$ = 166 $\pm$ 1 nM). These results also are consistent with PAT rank order of affinity functional in CHOgpH$_1$ and CHOhuH$_1$ cells (Table 1), rat brain (Choksi et al., 2000), and guinea pig brain (Bucholtz et al., 1998).

H_1-Mediated Contraction of Guinea Pig Ileum. As shown in Fig. 9, histamine (in absence of competing ligand) produced a concentration-dependent contraction of guinea pig ileum intestinal smooth muscle, with maximal effect occurring at about 10 μM histamine (EC$_{50}$ = 0.1 μM). Previously, it has been reported that this effect of histamine is mediated by H_1 receptors coupled to PLC and formation of IP and is competitively inhibited by H_1 antagonists (Leurs et al., 1991). Accordingly, based on the results here that $(-)$-*trans*-H$_2$-PAT antagonizes histamine-induced accumulation of [^{3}H]IP in CHOgpH$_1$ cells (vide supra), we assessed the ability of $(-)$-*trans*-H$_2$-PAT to act as an antagonist in the ileum

contraction assay. At concentrations spanning 0.01 to 10 μM, $(-)$-*trans*-H$_2$-PAT had no effect on contraction of guinea pig ileum (data not shown). Meanwhile, $(-)$-*trans*-H$_2$-PAT competitively antagonized the stimulation produced by histamine, producing rightward shifts of the histamine concentration-response curve with increasing concentrations of $(-)$-*trans*-H$_2$-PAT (Fig. 9); Schild regression analysis slope = 0.90 $\pm$ 0.01; pA_2 = 9.2.

Discussion

Previously, $(-)$-*trans*-H$_2$-PAT was shown to activate stereospecifically H_1 receptors coupled to modulation of tyrosine hydroxylase activity in guinea pig and rat forebrain in vitro (Booth et al., 1999) and in vivo (Choksi et al., 2000). Meanwhile, in brain tissue homogenates from these same species, the novel radioligand [^{3}H]$(-)$-*trans*-H$_2$-PAT labels only a subpopulation of the total number of H_1 receptors labeled by the standard antagonist H_1 radioligand [^{3}H]mepyramine (Booth et al., 1999; Choksi et al., 2000). In this article, we were able to more discretely examine the H_1 recognition features and associated functional activity of H$_2$-PAT by using cellular (CHO, COS) and tissue (guinea pig ileum strips) systems that are less complex than mammalian brain tissue.

The pharmacological profile of [^{3}H]$(-)$-*trans*-H$_2$-PAT labeled H_1 receptors in CHOgpH$_1$ and CHOhuH$_1$ cell membranes is similar to results obtained using the H_1 antagonist radioligand [^{3}H]mepyramine. For instance, the rank order of stereoselective affinity of several known H_1 ligands and H$_2$-PAT isomers for H_1 receptors labeled by [^{3}H]$(-)$-*trans*-H$_2$-PAT and [^{3}H]mepyramine (Table 1) is nearly identical. However, the current studies show that the number of H_1 receptors labeled by [^{3}H]$(-)$-*trans*-H$_2$-PAT in CHOgpH$_1$ and CHOhuH$_1$ cells is only about 15% of that labeled by [^{3}H]mepyramine. These results are similar to those obtained using rat brain tissue (Choksi et al., 2000). Meanwhile, in guinea pig brain the B_{max} for [^{3}H]$(-)$-*trans*-H$_2$-PAT is about 50% the value for [^{3}H]mepyramine (Booth et al., 1999)—the difference in rat versus guinea pig brain probably reflects the known species heterogeneity regarding the binding parameters of [^{3}H]mepyramine (Chang et al., 1979). In any case, it remains apparent that [^{3}H]$(-)$-*trans*-H$_2$-PAT generally labels only a fraction (about 15 to 50%) of the total histamine H_1 receptor population labeled by [^{3}H]mepyramine using
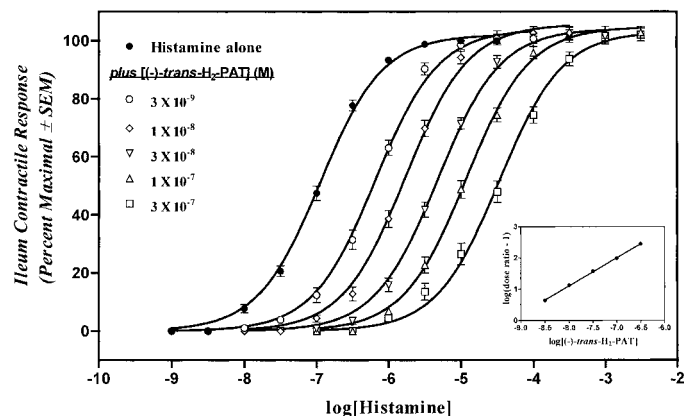
Fig. 9. H_1 receptor-mediated contraction of guinea pig ileum by histamine (maximal contraction at 10 μM; EC$_{50}$ = 0.1 μM) in absence and presence of competitive antagonist $(-)$-*trans*-H$_2$-PAT (pA_2 = 9.2).

either rodent brain tissue or clonal cell lines stably transfected with H₁ cDNA.

Initially, we hypothesized that $[^3H](-)$-*trans*-H₂-PAT may be an agonist-type radioligand that recognizes only a subpopulation of H₁ receptors in a high-affinity state (already coupled to G protein), whereas the H₁ antagonist radioligand $[^3H]$mepyramine may recognize both high- and low-affinity (i.e., not already coupled to G protein) H₁ receptors. This hypothesis is consistent with the H₁-mediated functional effect of $(-)$-*trans*-H₂-PAT to activate tyrosine hydroxylase and catecholamine synthesis similarly to the endogenous agonist histamine in vitro (Marley and Robotis, 1998) and in vivo (Fleckenstein et al., 1993). However, results of functional assays conducted here, using CHOgpH₁ and COShuH₁cells, clearly indicate that the pharmacology of H₂-PAT is similar to H₁ antagonists or inverse agonists, such as triprolidine (Fig. 7), mepyramine (Fig. 8), and acrivastine (Fig. 8), rather than the endogenous H₁ agonist histamine (Figs. 7 and 8). Moreover, $(-)$-*trans*-H₂-PAT potently antagonizes histamine-induced H₁-mediated contractile effects in guinea pig ileum (Fig. 9). Finally, binding potency of $(-)$-*trans*-H₂-PAT was unaffected (similar to the H₁ antagonist [+]-chlorpheniramine) in CHOgpH₁ cell membranes where virtually all the H₁ receptors were presumed to be uncoupled to G protein as a result of excess GTP; in contrast, histamine showed the lower binding potency (~50% decrease; Table 1) expected in systems where agonist ligand-receptor interaction is sensitive to the so-called GTP-shift. Results of the GTP-shift studies were the same regardless of whether $[^3H](-)$-*trans*-H₂-PAT or $[^3H]$mepyramine was used as the radioligand. Taken together, these results indicate that the fewer number of H₁ receptors labeled by $[^3H](-)$-*trans*-H₂-PAT versus $[^3H]$mepyramine in CHOgpH₁ and CHOhuH₁ cells probably is not due to differences in binding that result from differences in ligand-receptor functional interaction. Thus, we conclude that $(-)$-*trans*-H₂-PAT is not an agonist ligand (rather, it is an antagonist/inverse agonist) at H₁ receptors coupled to PLC/IP formation.

Meanwhile, H₁ receptors also can mediate histamine-induced stimulation of cAMP formation in mammalian brain (Palacios et al., 1978) and adrenal cells (Marley et al., 1991), and it has long been known that cAMP-dependent protein kinase A can activate tyrosine hydroxylase (Morgenroth et al., 1975). As the potency and efficacy of histamine to stimulate cAMP formation and tyrosine hydroxylase activity in bovine adrenal cells is similar, it is suggested H₁ receptors may modulate catecholamine synthesis via this pathway. Multifunctional signaling is apparent for many GPCR systems (Milligan, 1993), and this phenomenon has been described as "receptor promiscuity"—an unfaithfulness of a receptor to any one G protein (Kenakin, 1995a). Implicit in the receptor promiscuity hypothesis is the concept that a ligand that acts as an agonist at a receptor coupled to one particular signal transduction pathway may be an antagonist at the same receptor coupled to another signaling pathway. This phenomenon was termed "functional selectivity" to describe the effects of dopamine D₂ receptor ligands that are agonists at postsynaptic D₂ receptors but antagonists at presynaptic D₂ receptors (Ghosh et al., 1996). Receptor promiscuity and functional selectivity merge with the phenomenon of "precoupling of receptor-G protein complexes" (Leff and Scaramellini, 1998). Such spontaneous receptor-G protein

precoupling explains observed GPCR constitutive activity now abundantly documented, including for H₁ receptors (Bakker et al., 2000a,b). A critical assumption of these theories is that a heterogeneity of active receptor conformations exists and that agonists differ in their ability to induce, stabilize, or select among receptor conformations, as described in the "agonist trafficking" hypothesis (Kenakin, 1995b). Thus, a compelling body of theoretical and experimental evidence exists to suggest the hypothesis that $(-)$-*trans*-H₂-PAT could behave as an H₁ agonist or antagonist, depending on the associated signal transduction pathway, as influenced by ligand stabilization of particular H₁-G protein coupling. We note that this phenomenon may involve differences between pre- and postsynaptically expressed H₁ receptors (presynaptic neuronal H₁ receptors seem to be involved in modulation of brain catecholamine synthesis); thus, our future studies will include adrenal cells to measure postsynaptic H₁-mediated effects on tyrosine hydroxylase activity as we further test the proposed H₁ functional selectivity of $(-)$-*trans*-H₂-PAT.

Our finding that $(-)$-*trans*-H₂-PAT can fully displace $[^3H]$mepyramine binding to H₁ receptors in CHOhuH₁ membranes (Fig. 5) (and vice versa) seems to be at odds with results indicating $[^3H](-)$-*trans*-H₂-PAT labels only a fraction (about 15–50%, depending on the species) of the total H₁ receptors labeled by $[^3H]$mepyramine. This situation, however, is not unique among GPCRs. For example, the B_{max} for the dopamine D₂ receptor radioligand $[^3H]$spiperone has been known for some time to be severalfold lower than that for the D₂ radioligand $[^3H]$nemonapride; however, spiperone fully displaces $[^3H]$nemonapride, and nemonapride fully displaces $[^3H]$spiperone (Seeman et al., 1992). Subsequently, it was determined that the D₂ photoaffinity probe $[^{125}I]$-azidophenethyl-spiperone labels only D₂ monomers, whereas the D₂ photoaffinity probe $[^{125}I]$-azido-nemonapride labels both D₂ monomers and oligomers (Zawarynski et al., 1998). Apparently, radioreceptor experiments using reversible ligands with similar apparent K_D values do not distinguish subtle kinetic differences in GPCR monomer versus oligomer populations. Some other GPCR neurotransmitter systems for which single reversible radioligands did not predict monomer versus oligomer subpopulations but are now known to oligomerize include α_2 (Gouldson et al., 1997) and β_2 (Hebert et al., 1996) adrenergic, H₂ histamine (Fukushima et al., 1997), M₃ muscarinic (Maggio et al., 1999), and δ- and κ-opioid (Cvejic and Devi, 1997).

We speculate that H₁ receptors also may be expressed as monomers and oligomers. Previous studies using guinea pig brain membranes showed that a photoaffinity analog of mepyramine, $[^{125}I]$-iodoazidophenpyramine, labeled proteins of molecular weight 47, 56, 92, and 350 to 400 kDa (Ruat et al., 1988). Labeling of these proteins was prevented by an H₁ antagonist (the band at 92 kDa was only partially inhibited), suggesting these proteins were H₁-like. However, labeling of the 47-kDa protein also was diminished in the presence of protease inhibitors, suggesting it probably represented a proteolysis product. Meanwhile, labeling of the 350- to 400-kDa proteins greatly increased in the absence of 2-mercaptoethanol, suggesting these proteins to be higher molecular weight complexes linked by disulfide bridges. At the time, the 350- to 400-kDa proteins were interpreted as representing a 56-kDa H₁ receptor linked to one or more other (nondefined) peptides

or as artifactual disulfide linked peptides formed during membrane preparation (Ruat et al., 1988). In light of our results with $[^3H](-)$-*trans*-H_2-PAT and recent reports documenting a variety of GPCRs capable of oligomerization, we suggest that the proteins labeled by $[^{125}I]$-iodoazidophenpyramine in earlier studies may have been a combination of H_1 receptor monomers (i.e., 56 kDa) and oligomers (i.e., 350–400 kDa). In this regard, we believe $(-)$-*trans*-H_2-PAT represents a promising lead toward developing a (photo)affinity probe to differentiate H_1 receptor monomers from hypothesized H_1 oligomers and to determine whether GPCR oligomerization influences GPCR functional heterogeneity and vice versa.

References

Bakker RA, Schoonus SB, Smit MJ, Timmerman H, and Leurs R (2001) Histamine H_1-receptor activation of nuclear factor-κB: roles for G$\beta\gamma$- and G$\alpha_{q/11}$-subunits in constitutive and agonist-mediated signaling. *Mol Pharmacol* **60:**1133–1142.

Bakker RA, Wieland K, Timmerman H, and Leurs R (2000a) Constitutive activity of the histamine H_1 receptor reveals inverse agonism of histamine H_1 receptor antagonists. *Eur J Pharmacol* **387:**R5–R7.

Bakker RA, Wieland K, Timmerman H, and Leurs R (2000b) Constitutive activity of the histamine H_1 receptor reveals inverse agonism of histamine H_1 receptor antagonists. *Fundam Clin Pharmacol* **14:**44.

Booth RG, Owens CE, Brown RL, Bucholtz EC, Lawler CP, and Wyrick SD (1999) Putative σ_3 sites in mammalian brain have histamine H_1 receptor properties: Evidence from ligand binding and distribution studies with the novel H_1 radioligand $[^3H](-)$-*trans*-1-phenyl-3-aminotetralin (PAT). *Brain Res* **837:**95–105.

Booth RG, Wyrick SD, Baldessarini RJ, Kula NS, Myers AM, and Mailman RB (1993) New σ-like receptor recognized by novel phenylaminotetralins: ligand binding and functional studies. *Mol Pharmacol* **44:**1232–1239.

Brakenhoff RH, Knippels EM, and van Dongen GA (1994) Optimization and simplification of expression cloning in eukaryotic vector/host systems. *Anal Biochem* **218:**460–463.

Bucholtz EC, Wyrick SD, Owens CE, and Booth RG (1998) 1-Phenyl-3-dimethylaminotetralins (PATs): effect of stereochemistry on binding and function at brain histamine receptors. *Med Chem Res* **8:**322–332.

Chang RSL and Snyder SH (1980) Histamine H_1—receptor binding sites in guinea pig brain membranes: regulation of agonist interactions by guanine nucleotides and cations. *J Neurochem* **34:**916–922.

Chang RSL, Tran VT, and Snyder SH (1979) Heterogeneity of histamine H_1-receptors: species variations in $[^3H]$mepyramine binding of brain membranes. *J Neurochem* **32:**1653–1663.

Cheng YC and Prussof WH (1973) Relationship between the inhibition constant (K_i) and the concentration of inhibitor which causes 50% inhibition (IC_{50}) of an enzymatic reaction. *Biochem Pharmacol* **22:**3099–3108.

Choksi NY, Nix WB, Wyrick SD, and Booth RG (2000) A novel phenylaminotetralin recognizes histamine H_1 receptors and stimulates dopamine synthesis in vivo in rat brain. *Brain Res* **852:**151–160.

Cvejic S and Devi LA (1997) Dimerization of the δ-opioid receptor: implication for a role in receptor internalization. *J Biol Chem* **272:**26959–26964.

De Lean A, Stadel JM, and Lefkowitz RJ (1980) A ternary complex model explains the agonist-specific binding properties of the adenylate cyclase-coupled β-adrenergic receptor. *J Biol Chem* **255:**7108–7117.

Fleckenstein AE, Lookingland KJ, and Moore KE (1993) Activation of mesolimbic dopaminergic neurons following central administration of histamine is mediated by H_1 receptors. *Naunyn-Schmiedeberg's Arch Pharmacol* **347:**50–54.

Fukushima Y, Asano T, Saitoh T, Anai M, Funaki M, Ogihara T, Katagiri H, Matsuhashi N, Yazaki Y, and Sugano K (1997) Oligomer formation of histamine H_2 receptors expressed in Sf9 and COS-7 cells. *FEBS Lett* **409:**283–286.

Ghosh D, Snyder SE, Watts VJ, Mailman RB, and Nichols DE (1996) 8,9-Dihydroxy-2,3,7-11b-tetrahydro-1H-naph[1,2,3-de]isoquinoline: a potent dopamine D_1 agonist containing a rigid β-phenyldopamine pharmacophore. *J Med Chem* **39:**549–555.

Gouldson PR, Snell CR, and Reynolds CA (1997) A new approach to docking in the α_2-adrenergic receptor that exploits the domain structure of G-protein-coupled receptors. *J Med Chem* **40:**3871–3886.

Hebert TE, Moffett S, Morello JP, Loisel TP, Bichet DG, Barret C, and Bouvier M (1996) A peptide derived from a β2-adrenergic receptor transmembrane domain inhibits both receptor dimerization and activation. *J Biol Chem* **271:**16384–16392.

Kenakin T (1995a) Agonist-receptor efficacy I: mechanisms of efficacy and receptor promiscuity. *Trends Pharmacol Sci* **16:**188–192.

Kenakin T (1995b) Agonist-receptor efficacy II: agonist trafficking of receptor signals. *Trends Pharmacol Sci* **16:**231–238.

Leff P and Scaramellini C (1998) Promiscuity, pre-coupling and instability. *Trends Pharmacol Sci* **19:**13.

Leurs R, Brozius MM, Smit MJ, Bast A, and Timmerman H (1991) Effects of histamine H_1-, H_2- and H_3-receptor selective drugs on the mechanical activity of guinea-pig small and large intestine. *Br J Pharmacol* **102:**179–185.

Leurs R, Traiffort E, Arrang JM, Tardivel-Lacombe J, Ruat M, and Schwartz JC (1994) Guinea pig histamine H_1 receptor. II. Stable expression in Chinese hamster ovary cells reveals the interaction with three major signal transduction pathways. *J Neurochem* **62:**519–527.

Maggio R, Barbier P, Colelli A, Salvadori F, Demontis G, and Corsini GU (1999) G protein-linked receptors: pharmacological evidence for the formation of heterodimers. *J Pharmacol Exp Ther* **291:**251–257.

Marley PD and Robotis R (1998) Activation of tyrosine hydroxylase by histamine in bovine chromaffin cells. *J Autonomic Nervous System* **70:**1–9.

Marley PD, Thomson KA, Jachno K, and Johnston MJ (1991) Histamine-induced increases in cyclic AMP levels in bovine adrenal medullary cells. *Br J Pharmacol* **104:**839–846.

Milligan G (1993) Agonist regulation of cellular G protein levels and distribution: mechanisms and functional implications. *Trends Pharmacol Sci* **14:**413–418.

Morgenroth VH 3rd, Hegstrand LR, Roth RH, and Greengard P (1975) Evidence for involvement of protein kinase in the activation by adenosine 3′,5′-monophosphate of brain tyrosine 3-monooxygenase. *J Biol Chem* **250:**1946–1948.

Palacios JM, Garbarg M, Barbin G, and Schwartz JC (1978) Pharmacological characterization of histamine receptors mediating the stimulation of cyclic AMP accumulation in slices from guinea pig hippocampus. *Mol Pharmacol* **14:**971–982.

Ruat M, Korner M, Garbarg M, Gros C, Schwartz JC, Tertiuk W, and Ganellin CR (1988) Characterization of histamine H_1-receptor binding peptides in guinea pig brain using $[^{125}I]$iodoazidophenpyramine, an irreversible specific photoaffinity probe. *Proc Nat Acad Sci USA* **85:**2743–2747.

Seeman P, Guan HC, Civelli O, Van Tol HH, Sunahara RK, and Niznik HB (1992) The cloned dopamine D_2 receptor reveals different densities for dopamine receptor antagonist ligands. Implications for human brain positron emission tomography. *Eur J Pharmacol* **227:**139–146.

Smit MJ, Timmerman H, Hijzelendoorn JC, Fukui H, and Leurs R (1996) Regulation of the human histamine H_1 receptor stably expressed in Chinese hamster ovary cells. *Br J Pharmacol* **117:**1071–1080.

ter Laak AM, Timmerman H, Leurs R, Nederkoorn PH, Smit MJ, and Donne-Op KG (1995) Modelling and mutation studies on the histamine H_1-receptor agonist binding site reveal different binding modes for H1-agonists: Asp116 (TM3) has a constitutive role in receptor stimulation. *J Comput-Aided Mol Des* **9:**319–330.

Traiffort E, Leurs R, Arrang JM, Tardivel-Lacombe J, Diaz J, Schwartz J-C, and Ruat M (1994) Guinea pig histamine H_1 receptor. I. Gene cloning, characterization and tissue expression revealed by in situ hybridization. *J Neurochem* **62:**507–518.

Wyrick SD, Booth RG, Myers AM, Owens CE, Kula NS, Baldessarini RJ, and Mailman RB (1993) Synthesis and pharmacological evaluation of 1-phenyl-3-amino-1,2,3,4-tetrahydronaphthalenes as ligands for a novel receptor with σ-like modulatory activity. *J Med Chem* **36:**2542–2551.

Wyrick SD, Myers AM, Booth RG, Kula NS, Baldessarini RJ, and Mailman RB (1994) Sythesis of $[N$-$C^3H_3]$-*trans*-$(1R,3S)$-$(-)$-1-phenyl-3-*N,N*-dimethylamino-1,2,3,4-tetrahydronaphthalene (H_2-PAT). *J Lab Comp Radiopharm* **34:**131–134.

Zawarynski P, Tallerico T, Seeman P, Lee SP, O'Dowd BF, and George SR (1998) Dopamine D_2 receptor dimers in human and rat brain. *FEBS Lett* **441:**383–386.

Address correspondence to: Dr. Raymond G. Booth, Division of Medicinal Chemistry and Natural Products, School of Pharmacy, University of North Carolina at Chapel Hill, Chapel Hill, NC 27599-7360. E-mail: rbooth@email.unc.edu.